

Adaptive Control of Two-Mass Drive System with Nonlinear Stiffness

Abstract. The paper describes a nonlinear controller design technique for a servo drive in the presence of nonlinear friction together with a flexible shaft connecting the motor and the load. The shaft is characterized by the nonlinear stiffness curve. Two different type of the nonlinear stiffness curve are considered. The proposed controller is based on adaptive backstepping, modified by the use of command filtering. The proposed approach allows to accomplish the rigorous proof of the closed-loop system stability. Several experiments prove the control effectiveness.

Sterszczenie. Opisano problem sterowania prędkością układu napędowego z nieliniowym tarcie, połączeniem sprężystym i nieznanymi parametrami. Elastyczne połączenie jest opisane przy pomocy nieliniowej funkcji sztywności. Rozważane są dwa typy nieliniowej funkcji sztywności: wypukła i wklęsła. Układy regulacji są projektowane przy pomocy metod „adaptive backstepping” z filtracją wartości zadanych. Opisano szereg eksperymentów, które ilustrują charakterystyczne właściwości układu regulacji. (Adaptacyjne sterowanie dwu-masowego układu napędowego z nieliniową charakterystyką sztywności)

Keywords: nonlinear control, adaptive control, two-mass drive system, nonlinear stiffness.

Słowa kluczowe: sterowanie nieliniowe, sterowanie adaptacyjne, układy dwumasowe z połączeniem sprężystym, nieliniowa charakterystyka sztywności.

Introduction

Electric drive systems with elastic coupling between a motor and a load are common in various industrial applications: robotics, servo systems, paper- and textile machines, molding machines, and many others. It is well recognized that even the small coupling elasticity leads to mechanical resonances, and may cause failures and damages, that takes much time and cost to replace. The unnecessary shaft oscillations also destroy the control system dynamical performance and accuracy. Therefore the attenuation of torsional oscillations is the main problem for drives with an elastic coupling. Several control methods are used to design controllers for such drives: modifications of linear control techniques (PI, LQ, root locus, etc. – [1]), artificial neural networks [2], linear model predictive control [3-4], fuzzy controllers [5], nonlinear neural networks [6] and finally adaptive backstepping [7-9].

Despite different approaches, all these methods are based on the drive model which assumes that the torque transmitted by the shaft is proportional to the angle of torsion and the constant of proportionality, called “stiffness” is determined by the shaft material. The curve representing the torsion angle – transmitted torque characteristics, that will be called “a stiffness curve” is a straight line. This assumption is not correct in numerous drives if the shaft is constructed with the use of peculiar couplings. For example, if pneumatic couplings are used the stiffness curve is convex downward, strictly increasing [10-12]. In many drives, a flexible coupling with an elastic polymeric part is applied to compensate the axial eccentricity of the machines. In this case, the stiffness curve is concave downwards, strictly increasing as it is plotted in fig. 1 [13]. Actuators with nonlinear stiffness curve are common in numerous robotic applications [14-15].

Therefore, in this contribution, a nonlinear adaptive controller is proposed to cope with systems with nonlinear stiffness. Additionally, a static, nonlinear model of friction torques, which affect each end of the shaft are assumed. The designed controller is able to eliminate the shaft oscillations and to compensate the friction in presence of unknown system parameters.

Plant model and control objectives

The considered drive is modelled by four differential equations:

$$(1) \quad \begin{aligned} \dot{\varphi}_b &= \omega_b, \\ J_b \dot{\omega}_b &= kS(\varphi_r - \varphi_b) - T_b(\omega_b), \\ \dot{\varphi}_r &= \omega_r, \\ J_r \dot{\omega}_r &= -kS(\varphi_r - \varphi_b) - T_r(\omega_r) + T_m, \end{aligned}$$

where J_r corresponds to the inertia of the motor and J_b to the inertia of the load. The angular position of the motor is denoted by φ_r and the angular displacement of the load by φ_b . The drive torque coming from the motor T_m is the control input. The component $kS(\varphi_r - \varphi_b)$ represents the torque transmitted by the shaft.

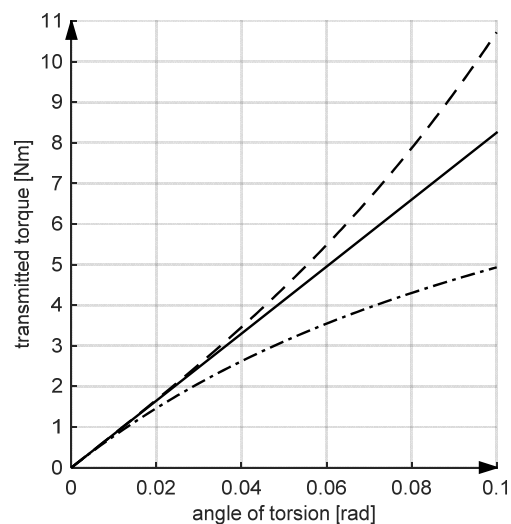


Fig.1. Different shapes of stiffness curves: solid line – linear, dotted – convex downward, dash-dotted – concave downward

The function S is assumed to be known and differentiable, while the constant coefficient k is unknown. The friction torques T_r and T_b are associated with J_r and J_b , respectively: T_b represents the load torque and the nonlinear frictional torques affecting the load-end of the drive and T_r stands for all frictional torques of the motor. It is convenient to separate the damping viscous friction component in $T_r(\omega_r)$ and $T_b(\omega_b)$:

$$(2) \quad \begin{aligned} T_b(\omega_b) &= c_b \omega_b + T_{fb}(\omega_b), \\ T_r(\omega_r) &= c_r \omega_r + T_{fr}(\omega_r), \end{aligned}$$

where c_r and c_b are the unknown, damping viscous coefficients associated with the motor and the load respectively. Functions $T_{fb}(\omega_b)$ and $T_{fr}(\omega_r)$ represent nonlinear components of friction torques associated with the Stribeck effect.

If the load velocity control is considered, the reduced model may be derived from the equations (1):

$$(3) \quad \varphi \stackrel{\text{def}}{=} \varphi_r - \varphi_b,$$

$$(4) \quad J_b \dot{\omega}_b = kS(\varphi) - T_b(\omega_b),$$

$$(5) \quad \dot{\varphi} = \omega_r - \omega_b,$$

$$(6) \quad J_r \dot{\omega}_r = -kS(\varphi) - T_r(\omega_r) + T_m.$$

The equation (5) may be replaced by

$$(7) \quad \frac{d}{dt}S(\varphi) = S'(\varphi)(\omega_r - \omega_b).$$

The model covers also the linear case when $S(\varphi) = \varphi$, $T_i(\omega_i) = c_i \omega_i$, $i = r, b$.

The control aim is to follow the smooth, desired load speed trajectory ω_{bd} .

Controller design

The adaptive controller is designed using the approach similar to adaptive backstepping [16]. The derivatives of the virtual controls will be obtained from linear filters, if necessary.

Step 1:

Consider the tracking error

$$(8) \quad e_b \stackrel{\text{def}}{=} \omega_b - \omega_{bd},$$

which is governed by the differential equation

$$(9) \quad \frac{J_b}{k} \dot{e}_b = -\frac{J_b}{k} \dot{\omega}_{bd} - \frac{T_b(\omega_b)}{k} + S(\varphi).$$

Because of the unknown parameters and nonlinearities in (9) it is assumed that the function $-\frac{J_b}{k} \dot{\omega}_{bd} - \frac{T_b(\omega_b)}{k}$ may be approximated by the linear-in-parameters model $\theta_b^T \xi_b$, where ξ_b are known functions and θ_b are unknown parameters. There are several possibilities to choose the approximation. For example the functions ξ_b may be selected as:

$$(10) \quad \xi_b^T = \left[-\frac{\bar{J}_b}{k} \dot{\omega}_{bd} \quad -\frac{\bar{c}_b}{k} \omega_b \quad -\frac{1}{k} \zeta_b^T(\omega_b) \right],$$

where:

- $\bar{\cdot}$ denotes the initial, approximate guess of the parameter \cdot ,
- components of $\zeta_b^T(\omega_b)$ constitute the basis (regressor) used to approximate $T_{fb}(\omega_b)$ from numerical data obtained from a steady-state friction characteristics.

Unavoidably, the approximation error ε_b occurs, such that

$$(11) \quad \theta_b^T \xi_b = -\frac{J_b}{k} \dot{\omega}_{bd} - \frac{T_b(\omega_b)}{k} - \varepsilon_b, \quad |\varepsilon_b| \leq \varepsilon_{bmax}.$$

The signal $S(\varphi)$ is so-called "virtual control" and is used to stabilize the equation (9). The desired value for the virtual control, so-called "stabilizing function" is denoted by α_b , and the tracking error is:

$$(12) \quad e_\varphi \stackrel{\text{def}}{=} S(\varphi) - \alpha_b.$$

Using all these notations in (9) results in

$$(13) \quad \frac{J_b}{k} \dot{e}_b = \theta_b^T \xi_b + \alpha_b + e_\varphi + \varepsilon_b.$$

The unknown parameters θ_b will be substituted by adaptive parameters $\hat{\theta}_b$ and the error of adaptation is denoted by

$$(14) \quad \tilde{\theta}_b \stackrel{\text{def}}{=} \theta_b - \hat{\theta}_b.$$

The choice

$$(15) \quad \alpha_b = -\hat{\theta}_b^T \xi_b - K_b e_b,$$

where $K_b > 0$ is the design parameter, results in

$$(16) \quad \frac{J_b}{k} \dot{e}_b = \tilde{\theta}_b^T \xi_b - K_b e_b + e_\varphi + \varepsilon_b.$$

Step 2:

The time-derivative of α_b is necessary to describe the dynamics of the error e_φ . Unfortunately, it requires differentiation of ξ_b and may produce complex mathematical expressions. Therefore this derivative is obtained from a first order filter:

$$(17) \quad \dot{z}_\varphi = -\alpha_\varphi (z_\varphi - \alpha_b), \quad z_\varphi(0) = \alpha_b(0).$$

The signal z_φ is the filter state variable and $\alpha_\varphi > 0$ is the filter design parameter, which decides how fast the steady state $z_\varphi = \alpha_b$ is achieved. It may be demonstrated that the filtering error remains bounded:

$$(18) \quad \rho_\varphi \stackrel{\text{def}}{=} z_\varphi - \alpha_b, \quad |\rho_\varphi| < \rho_{\varphi max}.$$

Defining the filtered tracking error

$$(19) \quad e_{\varphi f} \stackrel{\text{def}}{=} S(\varphi) - z_\varphi$$

allows to re-write (16) as

$$(20) \quad \frac{J_b}{k} \dot{e}_b = \tilde{\theta}_b^T \xi_b - K_b e_b + e_{\varphi f} + \rho_\varphi + \varepsilon_b.$$

The transient of $e_{\varphi f}$ is described by

$$(21) \quad \frac{d}{dt} e_{\varphi f} = S'(\varphi)(\omega_r - \omega_b) + \alpha_\varphi (z_\varphi - \alpha_b)$$

The signal ω_r is selected to be "virtual control" in (20), α_φ denotes the desired value for ω_r and

$$(22) \quad e_r \stackrel{\text{def}}{=} \omega_r - \alpha_\varphi.$$

Hence:

$$(23) \quad \frac{d}{dt} e_{\varphi f} = S'(\varphi)(e_r + \alpha_\varphi - \omega_b) + \alpha_\varphi (z_\varphi - \alpha_b).$$

Therefore, applying

$$(24) \quad \alpha_\varphi = \omega_b - \frac{1}{S'(\varphi)} [a_\varphi (z_\varphi - \alpha_b) + K_\varphi e_{\varphi f} + e_b] - \frac{1}{2} S'(\varphi) e_{\varphi f}$$

(where $K_\varphi > 0$ is the design parameter) provides:

$$(25) \quad \frac{d}{dt} e_{\varphi f} = S'(\varphi) e_r - K_\varphi e_{\varphi f} - e_b - \frac{1}{2} [S'(\varphi)]^2 e_{\varphi f}.$$

Step 3:

The same approach with the application of the filter, is repeated to obtain the next filtering error and its derivative. It is summarized by the following chain of expressions:

$$(26) \quad \dot{z}_r = -\alpha_r (z_r - \alpha_\varphi), \quad z_r(0) = \alpha_\varphi(0),$$

$$(27) \quad \rho_r \stackrel{\text{def}}{=} z_r - \alpha_\varphi, \quad |\rho_r| < \rho_{rmax},$$

$$(28) \quad e_r \stackrel{\text{def}}{=} \omega_r - \alpha_\varphi = \omega_r - z_r + z_r - \alpha_\varphi = e_{rf} + \rho_r,$$

$$(29) \quad e_{rf} \stackrel{\text{def}}{=} \omega_r - z_r.$$

Using these notations allows to re-write (25) as

$$(30) \quad \frac{d}{dt} e_{\varphi f} = S'(\varphi) e_{rf} + S'(\varphi) \rho_r - K_{\varphi} e_{\varphi f} - e_b - \frac{1}{2} [S'(\varphi)]^2 e_{\varphi f}.$$

The dynamics of the filtered error e_{rf} is given by

$$(31) \quad J_r \frac{d}{dt} e_{rf} = -kS(\varphi) - T_r(\omega_r) + J_r a_r(z_r - \alpha_{\varphi}) + T_m.$$

As in the first step, the function $-kS(\varphi) - T_r(\omega_r) + J_r a_r(z_r - \alpha_{\varphi})$ will be approximated by the linear-in-parameters model $\theta_r^T \xi_r$ with a bounded approximation error ε_r :

$$(32) \quad \theta_r^T \xi_r = -kS(\varphi) - T_r(\omega_r) + J_r a_r(z_r - \alpha_{\varphi}) - \varepsilon_r, \quad |\varepsilon_r| \leq \varepsilon_{rmax}.$$

Similarly as in (9,10), the model regressor may be selected as:

$$(33) \quad \xi_r^T = [-kS(\varphi) \quad -\bar{c}_r \omega_r \quad -\zeta_r^T(\omega_r) \quad \bar{J}_r a_r(z_r - \alpha_{\varphi})],$$

where, as previously, $\bar{\cdot}$ denotes the initial, approximate guess of the parameter \cdot and $\zeta_r^T(\omega_r)$ is the basis (regressor) used to approximate $T_{fr}(\omega_r)$.

Instead of the unknown parameters θ_r the adaptive parameters $\hat{\theta}_r$ are used and the adaptation error is denoted by:

$$(34) \quad \tilde{\theta}_r \stackrel{\text{def}}{=} \theta_r - \hat{\theta}_r.$$

The proposed control input

$$(35) \quad T_m = -\hat{\theta}_r^T \xi_r - K_r e_{rf} - S'(\varphi) e_{\varphi f}$$

(where $K_r > 0$ is the design parameter) results in the filtered error dynamics

$$(36) \quad J_r \frac{d}{dt} e_{rf} = -K_r e_{rf} + \tilde{\theta}_r^T \xi_r - S'(\varphi) e_{\varphi f} + \varepsilon_r.$$

System stability

The closed-loop system is described by the error equations (20), (30) and (36) and also includes the motion of the adaptive parameters, which must be designed to assure the whole system stability. The missing adaptive laws are derived by the analysis of the Lyapunov function

$$(37) \quad V = \frac{1}{2} \left(\frac{1}{k} e_b^2 + e_{\varphi f}^2 + J_r e_{rf}^2 + \tilde{\theta}_r^T \Gamma_r^{-1} \tilde{\theta}_r + \tilde{\theta}_b^T \Gamma_b^{-1} \tilde{\theta}_b \right).$$

The Lyapunov function derivative is calculated by the following chain of transformations:

$$(38) \quad \dot{V} = e_b (\hat{\theta}_b^T \xi_b - K_b e_b + e_{\varphi f} + \rho_{\varphi} + \varepsilon_b) + e_{\varphi f} [S'(\varphi) e_{rf} + S'(\varphi) \rho_r - K_{\varphi} e_{\varphi f} - e_b - \frac{1}{2} [S'(\varphi)]^2 e_{\varphi f}] + e_{rf} (-K_r e_{rf} + \tilde{\theta}_r^T \xi_r - S'(\varphi) e_{\varphi f} + \varepsilon_r) + \tilde{\theta}_r^T \Gamma_r^{-1} \frac{d}{dt} \tilde{\theta}_r + \tilde{\theta}_b^T \Gamma_b^{-1} \frac{d}{dt} \tilde{\theta}_b,$$

$$(39) \quad \dot{V} = -K_b e_b^2 - K_{\varphi} e_{\varphi f}^2 - K_r e_{rf}^2 + \tilde{\theta}_b^T (e_b \xi_b - \Gamma_b^{-1} \frac{d}{dt} \tilde{\theta}_b) + \tilde{\theta}_r^T (e_{rf} \xi_r - \Gamma_r^{-1} \frac{d}{dt} \tilde{\theta}_r) + e_b (\rho_{\varphi} + \varepsilon_b) - \frac{1}{2} [S'(\varphi)]^2 e_{\varphi f}^2 + e_{\varphi f} S'(\varphi) \rho_r + e_{rf} \varepsilon_r,$$

$$(40) \quad \dot{V} = -K_b e_b^2 - K_{\varphi} e_{\varphi f}^2 - K_r e_{rf}^2 + \tilde{\theta}_b^T (e_b \xi_b - \Gamma_b^{-1} \frac{d}{dt} \tilde{\theta}_b) + \tilde{\theta}_r^T (e_{rf} \xi_r - \Gamma_r^{-1} \frac{d}{dt} \tilde{\theta}_r) + e_b (\rho_{\varphi} + \varepsilon_b) - \frac{1}{2} [S'(\varphi)]^2 e_{\varphi f}^2 + e_{\varphi f} S'(\varphi) \rho_r - \frac{1}{2} \rho_r^2 + \frac{1}{2} \rho_r^2 + e_{rf} \varepsilon_r,$$

$$(41) \quad \dot{V} = -K_b e_b^2 - K_{\varphi} e_{\varphi f}^2 - K_r e_{rf}^2 + \tilde{\theta}_b^T (e_b \xi_b - \Gamma_b^{-1} \frac{d}{dt} \tilde{\theta}_b) + \tilde{\theta}_r^T (e_{rf} \xi_r - \Gamma_r^{-1} \frac{d}{dt} \tilde{\theta}_r) + e_b (\rho_{\varphi} + \varepsilon_b) - \frac{1}{2} (e_{\varphi f} S'(\varphi) - \rho_r)^2 + \frac{1}{2} \rho_r^2 + e_{rf} \varepsilon_r.$$

The adaptive laws are chosen as

$$(42) \quad \frac{d}{dt} \hat{\theta}_r = \Gamma_r (\xi_r e_{rf} - \sigma_r \hat{\theta}_r),$$

$$(43) \quad \frac{d}{dt} \hat{\theta}_b = \Gamma_b (\xi_b e_b - \sigma_b \hat{\theta}_b),$$

where σ_r, σ_b are positive constants.

Plugging (42) and (43) into (41) provides

$$(44) \quad \dot{V} = -K_b e_b^2 - K_{\varphi} e_{\varphi f}^2 - K_r e_{rf}^2 + e_b (\rho_{\varphi} + \varepsilon_b) - \frac{1}{2} (e_{\varphi f} S'(\varphi) - \rho_r)^2 + \sigma_b \tilde{\theta}_b^T \tilde{\theta}_b + \sigma_r \tilde{\theta}_r^T \tilde{\theta}_r + \frac{1}{2} \rho_r^2 + e_{rf} \varepsilon_r.$$

Making use of the inequalities

$$(45) \quad e_b (\rho_{\varphi} + \varepsilon_b) \leq \frac{1}{2} e_b^2 + \frac{1}{2} (\rho_{\varphi} + \varepsilon_b)^2,$$

$$(46) \quad e_{rf} \varepsilon_r \leq \frac{1}{2} e_{rf}^2 + \frac{1}{2} \varepsilon_r^2,$$

$$(47) \quad \tilde{\theta}_i^T \tilde{\theta}_i \leq \frac{1}{2} \tilde{\theta}_i^T \tilde{\theta}_i + \frac{1}{2} \theta_i^T \theta_i, \quad i = b, r,$$

leads to

$$(48) \quad \dot{V} \leq - \left(K_b - \frac{1}{2} \right) e_b^2 - K_{\varphi} e_{\varphi f}^2 - \left(K_r - \frac{1}{2} \right) e_{rf}^2 - \frac{\sigma_b}{2} \tilde{\theta}_b^T \tilde{\theta}_b - \frac{\sigma_r}{2} \tilde{\theta}_r^T \tilde{\theta}_r + \frac{\sigma_b}{2} \theta_b^T \theta_b + \frac{\sigma_r}{2} \theta_r^T \theta_r + \frac{1}{2} \rho_r^2 - \frac{1}{2} (\rho_{\varphi} + \varepsilon_b)^2 + \frac{1}{2} \varepsilon_r^2 \leq -K_{min} \|e\|^2 - \frac{\sigma_{min}}{2} \|\tilde{\theta}\|^2 + \varepsilon,$$

where $\varepsilon \stackrel{\text{def}}{=} \frac{\sigma_b}{2} \theta_b^T \theta_b + \frac{\sigma_r}{2} \theta_r^T \theta_r + \frac{1}{2} \rho_r^2 + \frac{1}{2} \varepsilon_r^2$, $K_{min} = \min \left(K_b - \frac{1}{2}, K_{\varphi}, K_r - \frac{1}{2} \right)$, $\sigma_{min} \stackrel{\text{def}}{=} \min(\sigma_b, \sigma_r)$, $e \stackrel{\text{def}}{=} [e_b, e_{\varphi f}, e_{rf}]^T$, $\tilde{\theta} \stackrel{\text{def}}{=} [\tilde{\theta}_b, \tilde{\theta}_r]^T$.

Finally, $\dot{V} < 0$ for $\|e\| \geq \sqrt{\frac{\varepsilon}{K_{min}}}$ and any $\|\tilde{\theta}\|$. On the other

hand, $\dot{V} < 0$ for $\|\tilde{\theta}\| \geq \sqrt{\frac{2\varepsilon}{\sigma_{min}}}$ and any $\|e\|$.

Concluding: under the proposed control the adaptive parameters error are uniformly ultimately bounded (UUB) [17] to the set:

$$(49) \quad P \stackrel{\text{def}}{=} \left\{ \tilde{\theta}: \|\tilde{\theta}\| \leq \sqrt{\frac{2\varepsilon}{\sigma_{min}}} \right\}$$

and the trajectories of the system (20), (30), (36) are uniformly ultimately bounded to the set:

$$(50) \quad Q \stackrel{\text{def}}{=} \left\{ e: \|e\| \leq \sqrt{\frac{\varepsilon}{K_{min}}} \right\}$$

and the bound for $\|e\|$ may be tighten by increasing K_i .

It follows directly from the filter equations that e_{φ} is bounded if $e_{\varphi f}$ is bounded and e_r is bounded if e_{rf} is bounded. The design parameters α_{φ}, a_r influence the transient speed and the level of the bound. Therefore the system of state variables $\bar{e} = [e_b \quad e_{\varphi} \quad e_r]^T$ is also UUB.

The derived controller is defined by the control law (35), adaptive laws (42,43) and the errors $e_{rf}, e_{\varphi f}, e_b$ are the controller inputs. The controller takes into account the nonlinearity of the stiffness curve: the function $S(\varphi)$ is used in the regressor ξ_r (35), in the error definitions (12, 19), and the derivative $S'(\varphi)$ is applied to the control (35) and in the stabilizing function (24). The adaptive loop keeps tuning the parameters including this one which corresponds to the gain k of $S(\varphi)$. The system is able to work properly if the stiffness model $S(\varphi)$ is not accurate, even if the linear stiffness is assumed, as long as the modelling errors remain bounded as it is assumed in (32). But the model including the nonlinear characteristics $S(\varphi)$ is more accurate, so it minimizes the effort of the adaptive loop and improves the system performance.

Simulation experiments

The characteristic features of the propose approach are investigated by simulation of an exemplary drive with parameters (in SI units) $J_1 = 0,4$, $b_1 = 4 \cdot 10^{-3}$, $k = 82,5$, $c_b = 0,1$, $c_r = 0,01$.

The simulations are done for two different function $S(\varphi)$:

- the stiffness curve is a convex downward, strictly increasing

$$(51) \quad S(\varphi) = \varphi + 30\varphi^3$$

- the stiffness curve is concave downwards, strictly increasing

$$(52) \quad S(\varphi) = \left(\frac{1}{3} + \frac{2}{3}e^{-9,242\varphi}\right)\varphi$$

The nonlinear components of friction torques $T_{fb}(\omega_b)$ and $T_{fr}(\omega_r)$ are given by

$$(53) \quad T_{fi} = \left(f_{si} + (f_{ci} - f_{si})e^{-\left(\frac{\omega_i}{\omega_{si}}\right)^2}\right) \tanh(100\omega_i), i = r, b$$

with the parameters $f_{sb} = 1$, $f_{sr} = 1$, $f_{cb} = 2$, $f_{cr} = 2$, $\omega_{sb} = \omega_{sr} = 0,03$.

The regressor functions ξ_b, ξ_r and vectors of unknown parameter θ_b, θ_r are defined as

$$(54) \quad \xi_b^T = \begin{bmatrix} -\dot{\omega}_{bd} & -\omega_b & -\tanh(100\omega_b) & -e^{-\left(\frac{\omega_b}{\omega_{sb}}\right)^2} \tanh(100\omega_b) \end{bmatrix}$$

$$(55) \quad \xi_r^T = \begin{bmatrix} -S(\varphi) & -\omega_r & -\tanh(100\omega_r) & -e^{-\left(\frac{\omega_r}{\omega_{sr}}\right)^2} \tanh(100\omega_r) & a_r(z_r - \alpha_\varphi) \end{bmatrix}$$

$$(56) \quad \theta_b^T = \left[\frac{J_b}{k} \quad \frac{c_b}{k} \quad \frac{f_{sb}}{k} \quad \frac{f_{cr} - f_{sr}}{k} \right]$$

$$(57) \quad \theta_r^T = [k \quad c_r \quad f_{sr} \quad f_{cr} - f_{sr} \quad J_r].$$

The desired output trajectory is given as:

$$(58) \quad \omega_{bd} = \sin(3t).$$

The controller parameters are chosen as: $K_b = 15$, $K_r = 15$, $K_\varphi = 15$, $\sigma_b = \sigma_r = 0,001$, $a_b = a_r = 10^4$, $\Gamma_b = [25 \ 250 \ 25 \ 25]$, $\Gamma_r = [0,25 \ 25 \cdot 10^5 \ 250 \ 25 \ 25]$.

The main aim of the conducted experiments was to compare two control algorithms:

1. taking into account the nonlinear stiffness curve $S(\varphi)$;
2. taking into account only the linear part of curve $S(\varphi)$, therefore assuming that

$$(59) \quad S(\varphi) \cong \varphi, S'(\varphi) \cong 1$$

instead of (51) or (52).

First, the non-adaptive case was investigated. It was assumed that all parameters of the plant are known exactly and the adaptation was switched off ($\Gamma_b = 0$, $\Gamma_r = 0$). As it is demonstrated in fig. 2 and fig. 6, the controller is able to stabilize the closed-loop system, although noticeable output oscillations are visible if the nonlinear part of the stiffness curve is not taken into account.

Next, the adaptive control was tested. The initial value of each component of vectors $\hat{\theta}_b, \hat{\theta}_r$ was approximated with 50% error. Again, the adaptive controller was able to stabilize the closed-loop system with nonlinear stiffness, using linear model of the stiffness curve. All state variables behave properly and the adaptive parameters are bounded. But it is visible that the quasi-steady-state oscillations of the

output are eliminated if the nonlinear model of the stiffness curve is used (fig. 3 and fig. 7). The adaptive loop effort is also much smaller in this case: significantly reduced amplitude of oscillations of adaptive parameters was observed (fig. 4,5, fig. 8,9).

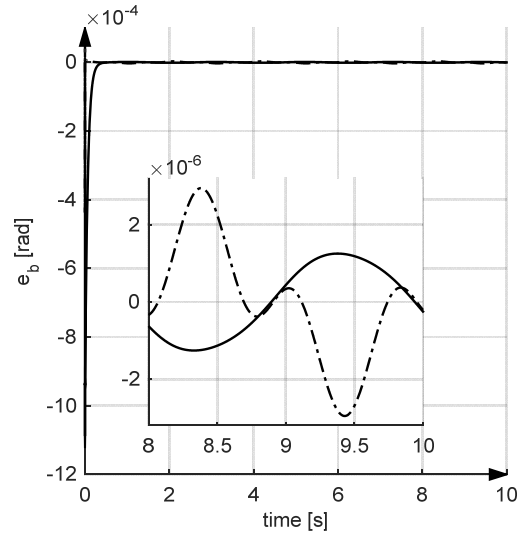


Fig.2. The tracking error e_b for a convex stiffness curve with the non-adaptive controller: solid line – case 1; dash-dotted – case 2

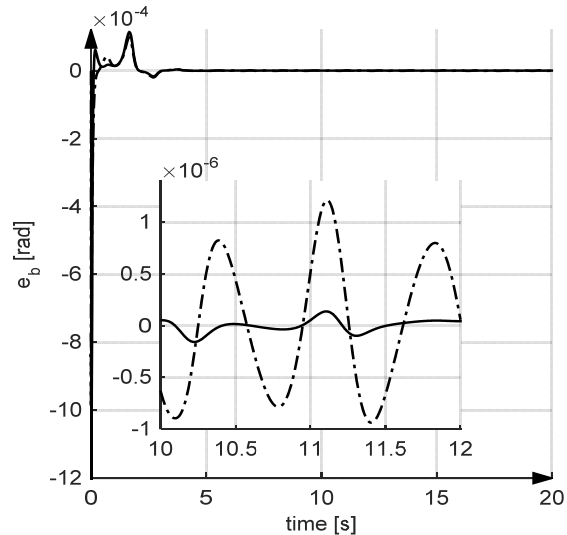


Fig.3. The tracking error e_b for a convex stiffness curve with the adaptive controller: solid line – case 1; dash-dotted – case 2

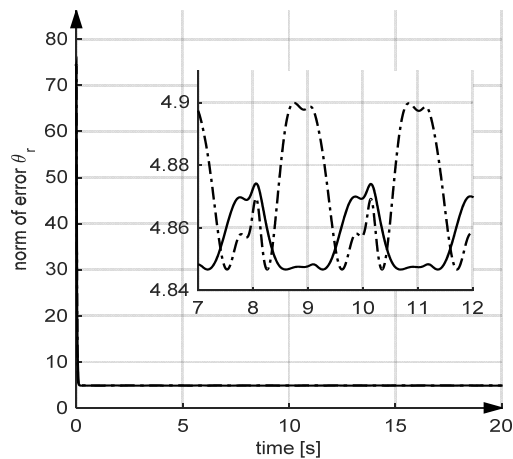


Fig.4. The norm of error adaptive parameters $\|\hat{\theta}_b\|$ for a convex stiffness curve: solid line – case 1; dash-dotted – case 2

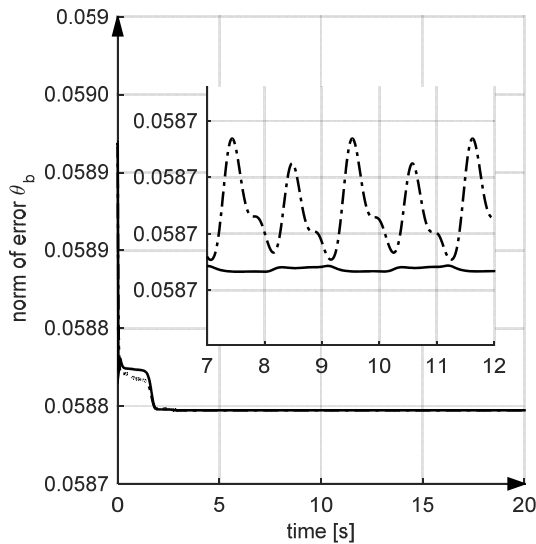


Fig.5. The norm of error adaptive parameters $\|\tilde{\theta}_r\|$ for convex stiffness curve: solid line – case 1; dash-dotted – case 2

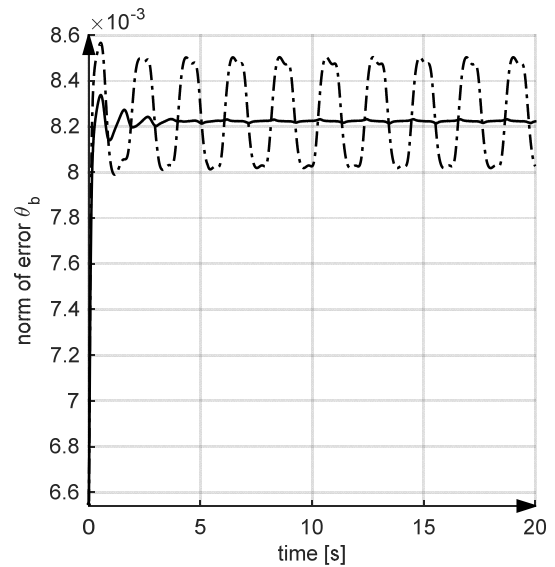


Fig.8. The norm of error adaptive parameters $\|\tilde{\theta}_b\|$ for a concave stiffness curve: solid line – case 1; dash-dotted – case 2

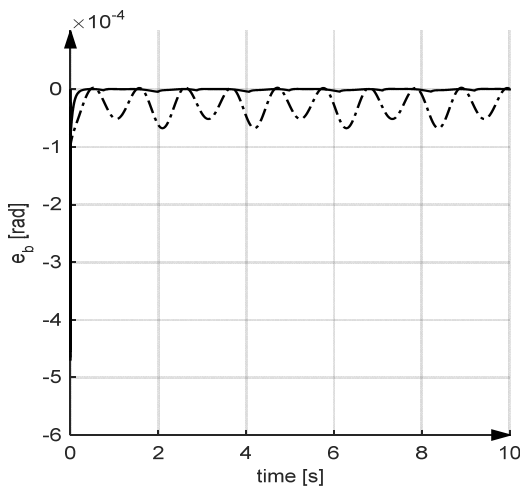


Fig.6. The tracking error e_b history for concave stiffness curve with non-adaptive controller: solid line – case 1; dash-dotted – case 2

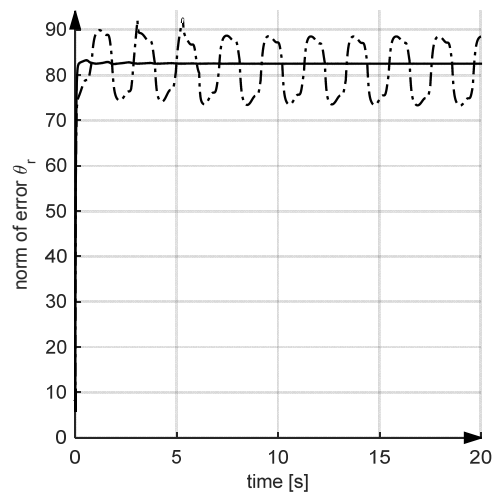


Fig.9. The norm of error adaptive parameters $\|\tilde{\theta}_r\|$ for a convex stiffness curve: solid line – case 1; dash-dotted – case 2

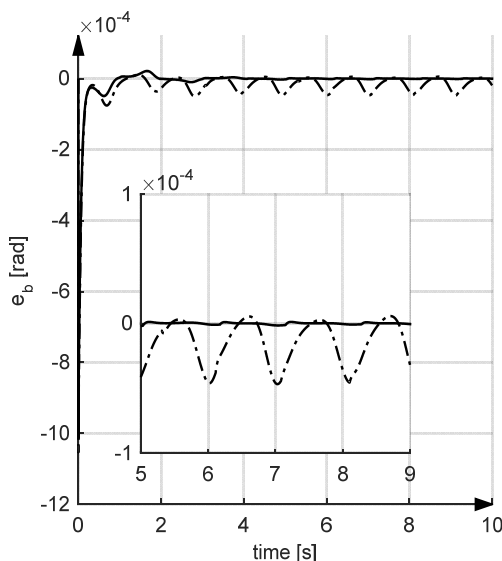


Fig.7. The tracking error e_b history for a concave stiffness curve with the adaptive controller: solid line – case 1; dash-dotted – case 2

Conclusions

First of all, the presented results demonstrate that the design of the adaptive controller for two-mass resonant systems with a nonlinear model of stiffness is possible. The design procedure is not complicated and the implementation demonstrates the same level of complexity as in a linear case. So, taking into account a nonlinear model of a stiffness curve is not “expensive” in any sense. As a “reward” a better control quality and a smaller effort of the adaptive loop are obtained.

The presented technique provides effective control of two-mass resonant systems with nonlinear stiffness. The same design approach is able to suppress the shaft oscillations and to compensate for nonlinear friction or any other resistance torques. The control is based on the command filtering adaptive backstepping (CFAB) approach. The CFAB techniques allow to perform the rigorous proof of the closed loop system stability in UUB sense. The derived controllers are not difficult to tune.

Authors: Jacek Kabziński D.Sc., Ph.D., E-mail: jacek.kabzinski@p.lodz.pl; Przemysław Mosiołek Ph.D., przemyslaw.mosiolek@p.lodz.pl; Lodz University of Technology, Institute of Automatic Control, ul. Stefanowskiego 18-22, 90-924 Łódź

REFERENCES

- [1] Szabat K., Kowalska T. O., Vibration suppression in a two-mass drive system using PI speed controller and additional feedbacks-comparative study, *IEEE Transactions on Industrial Electronics*, 54 (2007), n.2, 1193-1206
- [2] Orłowska-Kowalska T., Dybkowski M., Szabat K., Adaptive sliding-mode neuro-fuzzy control of the two-mass induction motor drive without mechanical sensor, *IEEE Transactions on Industrial Electronics*, 57 (2010), n.2, 553-563
- [3] Serkies P., Szabat K., Predictive position control of the induction two-mass system drive, IEEE 23rd International Symposium on Industrial Electronics (ISIE) (2014), 871-876
- [4] Serkies P., Szabat K., Application of the MPC to the Position Control of the Two-Mass Drive System, *IEEE Transactions on Industrial Electronics*, 60 (2013), 936-945
- [5] Fitri Y., Yasuchika M., Intelligent control method for two-mass rotary positioning systems, Proceedings of SICE Annual Conference (SICE) (2013), 2524-2529
- [6] Chaoui H., Sicard P., Lakhsasi A., Schwartz, H., Neural network based model reference adaptive control structure for a flexible joint with hard nonlinearities, IEEE International Symposium on Industrial Electronics, 1 (2004), 271-276
- [7] Kabziński J., Oscillations and Friction Compensation in Two-Mass Drive System with Flexible Shaft by Command Filtered Adaptive Backstepping, 1st Conference on Modelling, Identification and Control of Nonlinear Systems (MICNON-2015), 2015
- [8] Kabziński J., Mosiotek P., Adaptive Control of Nonlinear Resonant Systems with Damping, 20th International Conference on Methods and Models in Automation and Robotics (MMAR), (2015), 659-664
- [9] Kabziński J., Adaptive Control of Drillstring Torsional Oscillations, IFAC 2017 World Congress, Toulouse, France
- [10] Homisin J., Controlling torsional vibration of mechanical systems by application of pneumatic flexible shaft couplings, *Zeszyty Naukowe Transport, Politechnika Śląska* 72 (2011), 33-40
- [11] Abry F., Brun X., Sesmat S., Bideaux E., Ducat C., Electropneumatic Cylinder Backstepping Position Controller Design With Real-Time Closed-Loop Stiffness and Damping Tuning, *IEEE Transactions on Control Systems Technology*, 24 (2016), no.2,
- [12] Lee D. S., Choi D. H., A Dynamic Analysis of a Flexible Rotor in Ball Bearings with Nonlinear Stiffness Characteristics, *International Journal of Rotating Machinery*, 3 (1997), no.2, 73-80
- [13] Lijesh K. P., Harish H., Stiffness and damping coefficients for rubber mounted hybrid bearing, *Lubrication Science* 26 (2014), 301-314
- [14] Lan S., Song Z., Design of a New Nonlinear Stiffness Compliant Actuator and Its Error Compensation Method, *Journal of Robotics* 2016 (2016)
- [15] Petit F., Daasch A., Albu-Schäffer A., Backstepping Control of Variable Stiffness Robots, *IEEE Transactions On Control Systems Technology*, 23 (2015), no.6
- [16] Krstic, M., Kanellakopoulos, I., Kokotovic, P. V., Nonlinear and Adaptive Control Design, Wiley (1995)
- [17] Khalil H., Nonlinear Systems, Macmilan Publishing Co. (1992)